Fracture Mechanics of Concrete and Concrete Structures -
Recent Advances in Fracture Mechanics of Concrete - B. H. Oh, et al.(eds)
ⓒ 2010 Korea Concrete Institute, Seoul, ISBN 978-89-5708-180-8

Cohesive-force-based G_R crack extension resistance of concrete

X.F. Zhang & S.L. Xu
Dalian University of Technology, Dalian, P.R. China

ABSTRACT: This paper presents an investigation on a cohesive-force-based crack extension resistance curve of concrete determined in terms of energy release rate parameter, in which crack resistance denoted as G_R is composed of two parts. One part is crack fracture resistance contributed by hardening matrix. The second is fracture resistance contributed by aggregate cohesive bridging force. For the front, the value is considered to be a constant approximately equal to the fracture toughness of cement paste matrix. While for the latter, the value is related to post-cracking softening mechanical behavior of concrete. Numerical simulations are carried out on seven standard three point bending notched beams to examine the G_R curve as well as to investigate the effect of beam depth and concrete strength. The load-crack mouth opening displacement curve and initial cracking load are monitored in the simulation. Calculated results indicate that the fracture energy of specimen has significant impact on the G_R curve. Subsequently, a simplified trilinear model is proposed for G_R curve.

1 INTRODUCTION

The increase of crack fracture resistance of materials with the crack extension is often characterized by R-curve theory in fracture mechanics domain. Generally, R-curve is a function of structure geometry, materials fracture properties and crack propagation. The concept of R-curve was first introduced for fracture of metals (Irwin et al. 1960), in which a couple of equations were constructed to separately serve as the necessary and sufficient conditions to judge the incipient of unstable crack propagation.

For concrete materials, R-curve had been experimentally determined when the crack extension was measured (Hilsdorf & Brameshuber 1984, Mai 1984, Karihaloo 1987, Xu & Reinhardt 1999). However, it is almost impossible and impractical to accurate measure the position of crack tip in concrete materials. With this reason, various semi-experimental and semi-analytical ways were later developed to construct R-curve (Ouyang & Shah 1991, Bazant & Kazemi 1990). In their works, according to the definition proposed by authors (Irwin et al. 1960), R-curve was interpreted as a representation of an envelope of critical energy release rate for a series of structures. Although they considered the influence of fracture process zone on fracture behavior of concrete in their respective introduced material parameters, the contribution of aggregate bridging to crack fracture resistance is not clearly pointed out.

In 1999, a new solution to R-curve was analytically developed in combination with fictitious crack model(Hillerborg et al. 1976), in which R-curve was composed of two parts, i.e. crack resistance contributed by matrix and crack resistance offered by aggregate bridging action (Xu & Reinhardt 1998, 1999). Since stress intensity factor parameter was used in their model, R-curve was termed K_R crack resistance curve. Using three point bending notched beams, they investigated the fundamental characteristics of K_R crack resistance curve and analyzed crack stability. Recently, the K_R crack resistance curve was further extended from the view of energy using energy release rate parameter by Xu and Zhang, called G_R curve (Zhang 2007). The present paper was to present an introduction of the determination of G_R crack extension resistance curve. The influences of specimen sizes and concrete strengths on G_R curve were examined. The present work may be regarded as an extension of the research work on K_R crack resistance curve carried out by authors (Xu & Reinhardt 1998, Reinhardt & Xu 1999).

2 ANALYTICAL CALCULATION OF G_R CRACK EXTENSION RESISTANCE

2.1 *Theoretical model*

In the development of G_R crack extension resistance curve, energy release rate instead of stress intensity factor is utilized as analysis parameter. However, the superposition principle used in K_R crack extension resistance curve developed by Xu and Reinhardt (Xu & Reinhardt 1998, 1999) is considered to still hold true for G_R crack extension resistance curve. As a consequence, G_R crack extension resistance at arbitrary crack propagation time can be expressed as the sum of the contribution from matrix and one from aggregate bridging action. It is given by the following equation,

$$G_R(\Delta a) = G_{R-m} + G_{R-b} \tag{1}$$

in which, $G_{R\text{-}m}$ represents surface energy required for creating unit length crack in matrix; GR-b represents energy necessary for overcoming aggregate bridging force. In this analysis, matrix material is assumed to be an ideally linear elastic material. Accordingly, GR-m is taken constant, termed initiation fracture toughness GIcini. This means that when driving force offered by applied external load is less than initiation fracture toughness GIcini, no crack propagation occurs in matrix. Once initiation fracture toughness is exceeded, macro-crack begins to extend forward. However, this macro-crack is not stress-free. In reality, some cohesive force is distributed along this macro-crack due to aggregate bridging to prevent from the opening of crack. Often, the value of cohesive force is related to opening of crack and is described by traction-separation law. Therefore, GR-b is a function of the cohesive force shape $f(\sigma)$ and crack extension Δa. Thus, the G_R crack extension resistance can be further written as,

$$G_R(\Delta a) = G_{\mathrm{Ic}}^{\mathrm{ini}} + G_{R-b}\left(f(\sigma), \Delta a\right) \tag{2}$$

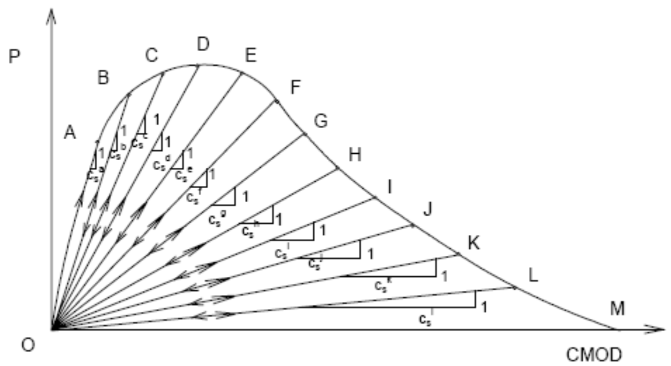

Figure 1. Linear asymptotic superposition assumption.

2.2 *Determination of effective crack propagation length*

In order to determine G_R crack resistance curve using Equation (2), the effective crack propagation length corresponding to arbitrary loading moment needs to be first known. In fracture of concrete, elastic equivalent approach is often used to simply nonlinear crack propagation in various models such as two-parameter fracture model (Jenq & Shah 1985), effective crack model (Karihaloo & Nallathambi 1990, Refai & Swartz 1987) and double-K fracture model (Xu & Reinhardt 1999). Herein, linear asymptotic superposition assumption proposed in double-K fracture model is adopted to calculate the length of effective crack propagation. In this assumption, an effective crack consists of an equivalent-elastic stress-free crack and an equivalent-elastic fictitious crack extension. Figure 1 demonstrates the sketch of linear asymptotic superposition assumption in terms of load-crack mouth opening displacement plot. According to this assumption, the nonlinear behavior on *P-CMOD* may be explained as an assembly of a series of linear points with the secant compliance of $C_s^{\,i}$. Thus, for three point bending beam geometry, the length of the effective crack a can be readily obtained by solving nonlinear Equation (3) using error and trial method (Tada et al. 1985).

$$C_\mathrm{s}^\mathrm{i} = \frac{24a}{BDE} V(a/D) \tag{3}$$

$$V(a/D) = 0.76 - 2.28a/D + 3.87(a/D)^2 - 2.04(a/D)^3 + 0.66/(1-a/D)$$

in which, B is beam width; D is beam depth; E is Young's modulus; $C_\mathrm{s}^\mathrm{i} = CMOD/P$ is secant compliance.

2.3 *Determination of $G_{R\text{-}b}$ crack resistance*

As mentioned above, cohesive fracture resistance $G_{R\text{-}b}$ is associated with softening property of concrete. Therefore, its value depends on traction-separation law used in the calculation. In the present paper, nonlinear relationship between cohesive force and opening of crack (Reinhardt et al. 1986) is adopted.

$$\frac{\sigma}{f_\mathrm{t}} = \left\{1 + \left(c_1 \frac{w}{w_0}\right)^3\right\} \exp\left(-c_2 \frac{w}{w_0}\right) - \frac{w}{w_0}\left(1 + (c_1)^3\right)\exp(-c_2) \tag{4}$$

where, f_t is tensile strength of concrete; c_1 and c_2 are two constants; w is opening of crack; σ is cohesive force corresponding to w; w_0 is maximum crack opening beyond which cohesive force is reduced down to zero. The value of w corresponding to any crack propagation x can be computed using Equation (5) (Jenq & Shah 1985).

$$w = CMOD\left\{\left(1 - \frac{x}{a}\right)^2 + \left(1.081 - 1.149\frac{a}{D}\right)\left[\frac{x}{a} - \left(\frac{x}{a}\right)^2\right]\right\} \tag{5}$$

Inserting $a=a_0$ into Equation (5), crack tip opening displacement, *CTOD*, can be obtained. Depending on the value of *CTOD*, two distinct stages during the complete fracture process should be distinguished in the determination of $G_{R\text{-}b}$.

Case I: $CTOD \le w_0$

Figure 2 shows the development of fracture process zone (FPZ) when the crack tip opening displacement $CTOD$ calculated from Equation (5) is less than the maximum crack opening w_0 of softening curve. Because of $CTOD \le w_0$, some cohesive force is distributed over the entire FPZ.

According to Figure 2, crack at the arbitrary position x of FPZ opens from zero to w_x. Correspondingly, cohesive bridging traction will reduce from f_t to $\sigma(w_x)$ according to softening relationship. Thus, energy consumed at the position x, termed local fracture energy $g_f(x)$, may be calculated from Equation (6), based on the definition of fracture energy (Hillerborg 1976).

$$g_f(x) = \int_0^{w_x} \sigma(w) dw \tag{6}$$

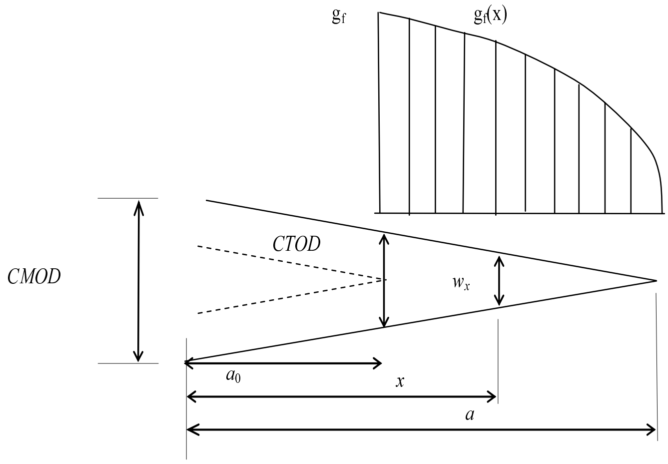

Figure 2. Distribution of local fracture energy along crack propagation when $CTOD \le w_0$.

Similarly, local fracture energy at other locations in FPZ can be calculated using Equation (6). Figure 2 shows the distribution of local fracture energy along FPZ. By integrating local fracture energy from a_0 to a, the energy dissipation corresponding to this crack extension can be determined by the expression as follows,

$$\Pi(x) = \int_{a_0}^{a} g_f(x) dx = \int_{a_0}^{a} \int_0^{w_x} \sigma(w) dw \tag{7}$$

According to the definition that $G_{R\text{-}b}$ is average energy dissipation for crack propagation $a - a_0$, Equation (8) can be then used to obtain $G_{R\text{-}b}$.

$$G_{R-b}(\Delta a) = \frac{\int_{a_0}^{a} \int_0^{w_x} \sigma(w) dw}{a - a_0} \tag{8}$$

Case II: $CTOD > w_0$

Figure 3 shows the development of fracture process zone (FPZ) when the crack tip opening displacement $CTOD$ calculated from Equation (5) is larger than the maximum crack opening w_0 of softening curve. In this Figure, a characteristic crack length a_{w0} at which crack opening is equal to w_0 is introduced. The value of a_{w0} can be obtained using Equation (5). According to traction-separation law, cohesive bridging force corresponding to arbitrary crack location in this range of a_{w0} - a_0 is reduced to zero from tensile strength f_t because the crack opening is larger than w_0. Therefore, in this range of a_{w0} - a_0, local fracture energy is equal to fracture energy G_f (see Equation (9)) given by Hillerborg. As a result, unchangeable local fracture energy is distributed over crack propagation of a_{w0} - a_0.

$$g_f(x) = \int_0^{w_0} \sigma(w) dw = G_f \tag{9}$$

whereas, in the range of $a - a_{w0}$, a rising local fracture energy is demonstrated as the crack is close to the initial crack tip, the same to Case I. Hence, in this case of $CTOD > w_0$, $G_{R\text{-}b}$ will be calculated using Equation (10).

$$G_{R-b}(\Delta a) = \frac{\int_{a_0}^{a} \int_0^{w_x} \sigma(w) dw}{a - a_0} + \frac{a_{w0} - a_0}{a - a_0} G_f \tag{10}$$

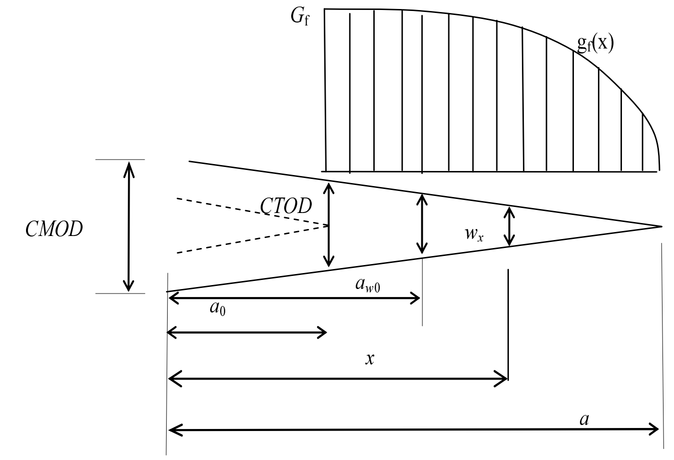

Figure 3. Distribution of local fracture energy along crack propagation when $CTOD > w_0$.

2.4 *Determination of G_{Ic}^{ini} crack resistance*

Because matrix material is assumed to be a brittle material, the expression for energy release rate in linear elastic fracture mechanics may be directly applied to calculate the value of $G_{\mathrm{Ic}}^{\mathrm{ini}}$. It is given by,

$$G_{\mathrm{Ic}}^{\mathrm{ini}} = \frac{\left(P^{\mathrm{ini}}\right)^2}{2B} \left.\frac{dC}{da}\right|_{a=a_0} \tag{11}$$

in which, P^{ini} is cracking load; $\mathrm{d}C/\mathrm{d}a$ is the differentia of compliance with respect to crack extension and can be gained using load-loading point displacement relationship (P-δ) as given in the following expression for three point bending beam (Xu & Zhang 2008).

$$\frac{dC}{da}=\frac{d}{da}\left(\frac{\delta}{P}\right)=\frac{3S^2}{2BD^3E}V'(\alpha_0) \quad (12)$$

$$V'(\alpha_0)=\frac{2\alpha_0}{(1-\alpha_0)^3}\left[5.58-19.57\alpha_0+36.82\alpha_0^2-34.94\alpha_0^3+12.77\alpha_0^4\right]$$
$$+\left(\frac{\alpha_0}{1-\alpha_0}\right)^2\left[-19.57+73.64\alpha_0-104.82\alpha_0^2+51.08\alpha_0^3\right]$$

in which, S is clear span of beam; α_0= initial crack length / beam depth ratio, a_0/D.

In addition, one can use the Equation (13) to evaluate the initial fracture toughness G_{Ic}^{ini}.

$$G_{Ic}^{ini}=\frac{\left(K_{Ic}^{ini}\right)^2}{E} \quad (13)$$

in which, K_{Ic}^{ini} = initiation fracture toughness expressed in form of stress intensity factor, which can be determined based on double-K fracture model (Xu & Reinhardt 1999, 2000).

Now, one can calculate G_R crack fracture resistance at any crack extension according to above procedures.

3 NUMERICAL SIMULATIONS

Seven notched standard three point bending beams were numerically simulated using a commercial nonlinear finite element procedure for reinforced concrete members. According to beam size and compressive strength of concrete, they were grouped into two series. In depth series, the beams have the same compressive strength of concrete. In strength series, beam size was kept constant, but the compressive strength of concrete was increased from 26.8MPa to 78.2MPa. The notch length/depth ratio was 0.3 for all beams investigated. Maximum size of coarse aggregates was 20mm in all concretes. The detailed sizes of beams and mechanical properties of concrete used were presented in Table 1.

Apart from fundamental material parameters given in Table 1, post-cracking properties of concrete, i.e. fracture energy and shape of softening stress-crack opening curve were needed in the input of numerical simulation in order to obtain the descending branch of the load versus crack mouth opening displacement curve. Herein, the nonlinear softening stress-crack opening curve was adopted, in which c_1=3.0, c_2=6.93, w_0=5.14G_f/f_t. Fracture energy G_f was determined from the compressive strength of concrete and maximum aggregate size of concrete according to the CEB-FIP Model Code 1990. The expression was written as,

$$G_f=\left(0.0204+0.0053{d_{\max}}^{0.95}/8\right)\left(f_c/f_{c0}\right)^{0.7} \quad (14)$$

in which $d_{\max}$ is maximum particle size of coarse aggregate, in mm; f_{c0} =10MPa. According to Equation (14), the parameters of nonlinear softening curve were determined for each beam, as listed in Table 2.

In practical simulation, four-node isoparametric element was used. The total number of elements and nodes was 654 and 714, respectively.

Table 1. Dimensions of specimens and material properties of concrete used.

Beams	$S \times D \times W$	f_c	f_t	E
	mm × mm × mm	*MPa*	*MPa*	*GPa*
M1BLH	1600×400×160	26.8	2.58	24.62
M1BMH	1200×300×120	26.8	2.58	24.62
M1BSH	800×200×80	26.8	2.58	24.62
M2BSH	800×200×80	39.0	3.11	33.80
M3BSH	800×200×80	49.4	3.50	34.65
M4BSH	800×200×80	67.5	4.09	37.20
M5BSH	800×200×80	78.2	4.41	40.30

Note: f_c=compressive strength.

Table 2. Parameters of softening curves.

Beams	G_f	f_t	w_0	c_1	c_2
	N/m	*MPa*	*μm*		
M1BLH					
M1BMH	63.42	2.58	126.34	3.0	6.93
M1BSH					
M2BSH	82.46	3.11	136.29	3.0	6.93
M3BSH	97.30	3.50	142.90	3.0	6.93
M4BSH	121.07	4.09	152.15	3.0	6.93
M5BSH	134.20	4.41	156.42	3.0	6.93

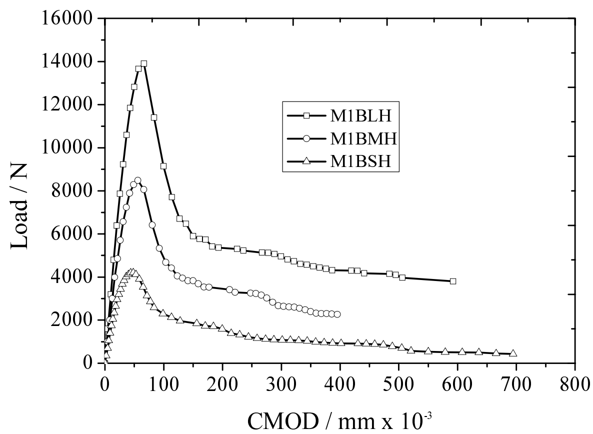

Figure 4. Load versus crack mouth opening displacement curves of specimens with different depths.

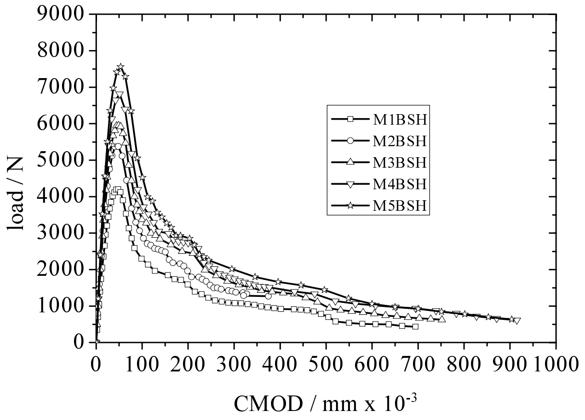

Figure 5. Load versus crack mouth opening displacement curves of specimens with various strengths.

The plots of load in terms of crack mouth opening displacement *CMOD* of specimens are shown in Figure 4 for depth series and in Figure 5 for strength series. The maximum load P_{max} and corresponding crack mouth opening displacement $CMOD_c$ were determined from Figure 4 and Figure 5, as summarized in Table 3. The calculated critical crack tip opening displacement $CTOD_c$ at P_{max} according to Equation (5) were listed in Table 3, too. At each load step, the distribution of tensile stress along the ligament of beam was examined. Specially, if tensile stress at the tip of the initial crack at certain load step reaches tensile strength of concrete, the initial crack begins to propagate. The load applied on beam corresponding to this load step was defined as initial cracking load P^{ini}. Table 3 gives the initial cracking load P^{ini} of beam tested.

As seen in Table 3, the ratio of initial cracking load to maximum load of each beam is roughly between 0.45 and 0.57. The averaged value of this ratio for all beams is 0.50, which is in agreement with the observation from uniaxial compressive tests of concrete where micro-crack is generally believed to cracking at 40%-50% of compressive strength.

Table 3. Initial cracking load, maximum load and critical crack opening.

Beams	P^{ini}	P_{max}	$CMOD_c$	$CTOD_c$	P^{ini} / P_{max}
	N	N	μm	μm	
M1BLH	7866	13907	66.46	25.94	0.566
M1BMH	4854	8586	56.14	22.64	0.565
M1BSH	2054	4200	47.98	21.32	0.489
M2BSH	2371	5377	48.20	22.29	0.441
M3BSH	2919	5954	48.83	21.82	0.490
M4BSH	3494	6816	51.12	22.61	0.513
M5BSH	3524	7559	53.50	23.96	0.466

4 RESULTS ANALYSIS

4.1 *Characteristics of G_R crack resistance curve*

Using the obtained *P-CMOD* curve and initial cracking load, G_R crack resistance curves are determined for seven specimens investigated in this study. Figure 6 and Figure 7 show the plots of G_R crack resistance in terms of crack extension a-a_0 for depth group and strength group, respectively. It can be seen that G_R curve of seven beams show the same trend, i.e. G_R first increases with development of crack until the characteristic effective crack propagation a_{w0} is reached and thereafter, G_R varies little, almost being a constant. Also, it is discovered from Figure 6 and Figure 7 that the value of G_R is comparable to fracture energy inputted in the calculation after a_{w0} is exceeded.

For three specimens with different depths, G_R curves overlap each other, showing no size-effect. While for strength series, specimen with higher concrete strength has higher G_R. In reality, as can be seen from Table 2, for depth group, three specimens have the same fracture energy, whereas for strength group, fracture energy differs greatly. Therefore, it is concluded that the G_R curve intensively depends on the value of fracture energy.

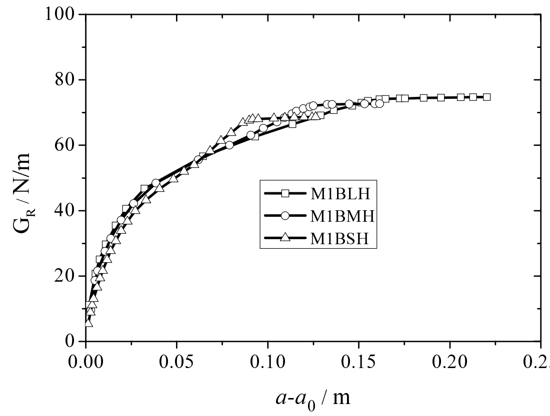

Figure 6. G_R crack resistance curves of specimens with different depths.

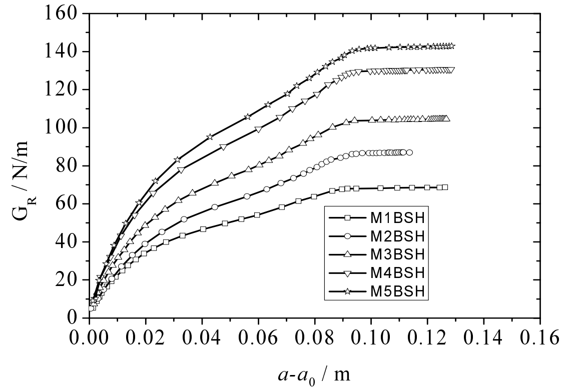

Figure 7. G_R crack resistance curves of specimens with different strengths.

4.2 *Simplified trilinear model*

As observed from Figure 6 and Figure 7, G_R of seven beams have the similar characteristics. It is noticed that G_R crack resistance curve can be simplified using a trilinear model. Herein, considering the length of this paper, only specimen M1BLH is taken as a demonstrative example (see Fig. 8). In Figure 8, the curve of load versus crack extension is included, too. Three controlling points, O, A and B on the trilinear model correspond to the onset of crack stable propagation, critical unstable propagation and crack propagation at which $w = w_0$, respectively. Therefore, G_R crack extension resistance can be also approximately simplified as,

$$\begin{cases} G_R(w) = k_1 \times \beta G_f & \text{for} \quad 0 \le w \le CTOD_c \\ G_R(w) = \beta G_f + k_2 \times \beta G_f & \text{for } CTOD_c \le w \le w_0 \\ G_R(w) = G_f & \text{for } w_0 \le w \end{cases} \tag{15}$$

where β = the ratio of critical unstable fracture resistance to fracture energy, in which critical unstable fracture resistance can be determined referring to the reference (Xu & Zhang 2008); $k_1 = w/CTOD_c$;

$k_2 = \dfrac{1-\beta}{\beta}\dfrac{w - CTOD_c}{w_0 - CTOD_c}$. $k_1\beta G_f$ and $k_2\beta G_f$ stand for the energy dissipation during the stage of stable crack propagation and unstable crack propagation, respectively. At $w = CTOD_c$, $k_1\beta G_f$ reaches its maximum value of βG_f while at $w = w_0$, $k_2\beta G_f$ does its maximum value of $(1-\beta)G_f$. Table 4 gives results of β and $CTOD_c/w_0$ for each beam.

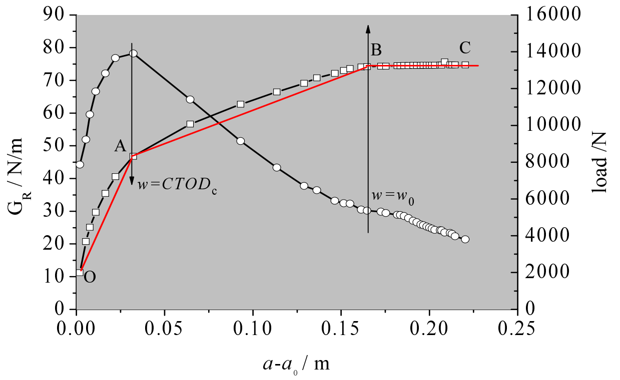

Figure 8. Trilinear model for G_R crack extension resistance.

Table 4. Values of β and CTODc/w0.

Beams	M1B LH	M1B MH	M1B SH	M2B SH	M3B SH	M4B SH	M5B SH
CTODc /w0	0.21	0.18	0.17	0.16	0.15	0.15	0.15
β	0.74	0.67	0.58	0.55	0.54	0.54	0.53

Results of Table 4 show that difference in either $CTOD_c/w_0$ or in β is negligible for beams with five concrete strengths. This means that the values of critical crack tip opening $CTOD_c$ and critical unstable fracture energy resistance G_{Ic}^{un} are proportional to w_0 and G_f, thereby relating to tensile strength because $w_0 = 5.14G_f/f_t$ is used in the simulations. Therefore, one can have

$$\frac{CTOD_c}{w_0} \propto \frac{G_{Ic}^{un}}{G_f} \Rightarrow \frac{CTOD_c}{G_{Ic}^{un}} = \frac{k_3}{f_t} \tag{16}$$

in which, k_3 is a coefficient. Substituting $K_{Ic}^{un} = \sqrt{EG_{Ic}^{un}}$ into Equation (16), one can have new expression for brittleness index Q.

$$Q = \frac{ECTOD_c}{\left(K_{Ic}^{un}\right)^2} = \frac{k_3}{f_t} \tag{17}$$

where, brittleness index Q is in MP-1, which differs from that defined in two-parameter fracture model(Jenq & Shah 1985) in which brittleness index Q is a material length with the unit of m. From Equation (17), it can be seen that the higher concrete strength, the smaller the brittleness index, the more brittle the material.

Regarding to specimens in depth group, the increase in depth will lead to an increase in both $CTOD_c/w_0$ and β. Furthermore, the tendency of a linear increase is demonstrated for β.

As can be seen in Table 4, all of seven beams have a β larger than 0.5. It means that for seven beams investigated the energy dissipation at stage of stable crack propagation is larger than that at the stage of unstable crack propagation.

5 CONCLUSIONS

Crack extension resistance curve during the entire process of concrete crack development is studied adopting energy release rate parameter. Analytical method to determine G_R curve is introduced. The calculated results of the numerical simulations on notched seven standard three point bending beams with various depths and strengths show the typical feature of G_R curve, i.e. it first increases as crack extends and then roughly converges to fracture energy. It also is shown that the value of G_R strongly depends on the value of fracture energy.

A simplified trilinear model for the proposed G_R curve is given. Critical crack tip opening $CTOD_c$, the maximum crack opening w_0 of softening curve, the critical unstable fracture resistance G_{Ic}^{un} and fracture energy are four controlling parameters on the simplified model. A new brittleness index is proposed. By preliminarily investigating these four parameters, it is concluded that concrete strength has little effect on $CTOD_c/w_0$ and $\beta = G_{Ic}^{un}/G_f$ while specimen depth shows some effect on them especially on $\beta = G_{Ic}^{un}/G_f$.

It is emphasized that, in the simulation, fracture energy inputted is based on CEB-FIP Model 1990 Code. This implies that, in the present investigation, fracture energy is independent of beam depth. More examinations on the influence of specimen geometry and size on the four controlling parameters are in progress.

REFERENCES

Bazant, Z.P. & Kazemi, M.T. 1990. Determination of fracture energy, process zone length and brittleness number from size effect, with application to rock and concrete. *International Journal of Fracture*, 44: 111-131.

Hillerborg, A et al. 1976. Analysis of crack formation and crack growth in concrete by means of fracture mechanics and finite elements. *Cement and Concrete Research*, 6: 773-782.

Hilsdorf, H.K. & Brameshuber, W. 1984. Size effects in the experimental determination of fracture mechanics parameters. In: *Shah S.P., editor. Application of fracture mechanics to cementitious composites*. NATO-ARW. 361-367.

Jenq, Y.S. & Shah, S.P. 1985. Two parameter fracture model for concrete. *Journal of Engineering Mechanics, ASCE*, 111: 1227-1241.

Karihaloo, B.L. 1987. Do plain and fiber reinforced concretes have an R-curve Behavior? *In Shah S.P. & Swartz S.E. editors. Fractures of concrete and rock*. Springer-Verlag, 96-105.

Karihaloo, B.L. & Nallathambi. 1990. Effective crack model for the determination of fracture toughness K_{Ic}^{s} of concrete. *Engineering Fracture Mechanics*, 35: 637-645.

Mai, Y.W. 1984. Fracture measurements of cementititous composites. In: *Shah S.P., editor. Application of fracture mechanics to cementitious composites*. NATO-ARW. 399-429.

Ouyang, C. & Shah, S.P. 1991. Geometry dependent R-curve for quasi-brittle materials. *Journal of the American Ceramic Society*, 74(11): 2831-2836.

Reports of Special ASTM Committee on fracture testing of high-strength metallic materials: fracture testing of high-strength sheet materials. ASTM Bulletin No.243, January 1960. 29-40.

Reinhardt, H.W. et al. 1986. Tensile tests and failure analysis of concrete. *Journal of Structural Engineering, ASCE*, 112: 2462-2477.

Swartz, S.E. & Refai, T.M.E. 1987. Influence of Size on Opening Mode Fracture Parameters for Precracked Concrete Beams in Bending. *Proceedings of SEM-RILEM International Conference on Fracture of Concrete and Rock (Edited by S.P. Shah and S.E. Swartz)*.Houston, Texas: 242–254.

Tada, H. et al. 1985. The stress analysis of cracks handbook. *St. Louis, Missouri. USA: Paris Productions Incorporated*.

Xu, S.L. & Reinhardt, H.W. 1998. Crack extension resistance and fracture propagation in quasi-brittle materials like concrete based on the complete process of fracture. *International Journal of Fracture*, 92: 71-99.

Xu, S.L. & Reinhardt, H.W. 1999. Determination of double-*K* criterion for crack propagation in quasi-brittle materials, part I: experimental investigation of crack propagation. *International Journal of Fracture* 98(2): 111–149.

Reinhardt, H.W. & Xu, S.L. 1999. Crack extension resistance based on cohesive force in concrete. *Engineering Fracture Mechanics*, 64: 563-587.

Xu, S.L. & Reinhardt, H.W. 1999. Determination of double-K criterion for crack propagation in quasibrittle materials, part II: analytical evaluating and practical measuring methods for three-point bending notched beams. *International Journal of Fracture* 98(2), 151–177.

Xu, S.L. & Reinhardt, H.W. 2000. A simplified method for determining double-K fracture parameters for three-point bending tests. *International Journal of Fracture*, 104: 181-208.

Xu, S.L. & Zhang, X.F. 2008. Determination of fracture toughness of concrete using energy approach. *Engineering Fracture Mechanics*. 75(15): 4292-4308.

Zhang, X.F. 2007. New G_R crack extension resistance and energy transformation analysis during the whole fracture process in concrete. *PhD. Thesis. Dalian University of Technology*.